$\bar{u}$ = local volume-averaged velocity of the solid; defined by Equation (11)
v = velocity
V = volume of S
$V_{(s)}$ = volume of pores containing fluid which are enclosed by the surface S

Greek letters

α, β, γ = parameters appearing in Equation (69)
ϵ = distance into an impermeable wall at which $\bar{\underset{\sim}{v}} = 0$
μ = viscosity
ρ = density
ϕ = external force potential; defined by Equation (5)
ψ = porosity

Special symbols

$\overline{\quad}$ = an average over the volume V of quantities associated with the fluid; see Equation (3)
* = a quantity associated with a new reference frame
$^+$ = a dimensionless variable
Λ = indicates a vector product

LITERATURE CITED

1. Slattery, J. C., *AIChE J.*, 13, 8, 1066 (1967).
2. *Ibid.*, 14, 50 (1968).
3. *Ibid.*, 5, 831 (1965).
4. *Ibid.*, 14, 516 (1968).
5. Truesdell, C., "The Elements of Continuum Mechanics," Springer-Verlag, New York (1966).
6. ———, and W. Noll, "Handbuch der Physik," III/3, S. Flügge, ed., Springer-Verlag, Berlin (1965).
7. Spencer, A. J., and R. S. Rivlin, *Arch. Rational Mech. Analysis*, 4, 214 (1959/60).
8. Smith, G. F., *ibid.*, 18, 282 (1965).
9. Brinkman, H. C., *Appl. Sci. Res.*, A1, 27, 81 (1949).
10. Irving, J., and N. Mullineux, "Mathematics in Physics and Engineering," Academic Press, New York (1959).
11. Truesdell, C., *Phys. Fluids*, 7, 1134 (1964).
12. Shertzer, C. R., and A. B. Metzner, *Proc. 4th Int. Congr. Rheol*, Pt. 2, 603 (1965).
13. Ginn, R. F., and A. B. Metzner, *ibid.*, 583 (1965).
14. McKinley, R. M., H. O. Jahns, W. W. Harris, and R. A. Greenkorn, *AIChE J.*, 12, 17 (1966).
15. Ashare, Edward, R. B. Bird, and J. A. Lescarboura, *ibid.*, 11, 910 (1965).
16. Christopher, R. H., MS thesis, Univ. Rochester, New York (1965).
17. Sadowski, T. J., Ph.D. thesis, Univ. Wisconsin, Madison (1963).

Manuscript received February 2, 1968; revision received July 8, 1968; paper accepted July 11, 1968. Paper presented at AIChE Tampa meeting.

Combined Forced and Free Convective Diffusion in Vertical Semipermeable Parallel Plate Ducts

KRISHNAN RAMANADHAN and WILLIAM N. GILL

Clarkson College of Technology, Potsdam, New York

The effect of natural convection on polarization and flow patterns in liquid phase convective diffusion in a vertical duct with semipermeable membrane walls has been investigated theoretically. It is found that at low flow rates, gravitational fields can play a significant role in distorting the velocity profiles and thereby they affect the transition from laminar to turbulent flow. Natural convection also significantly affects mass transfer rates and therefore the extent of polarization at low flow rates. Results are presented for both momentum and mass transfer in upward and downward flows for different wall Peclet numbers. The hydrodynamic stability of the system also has been investigated and critical values of the buoyancy parameters are reported. Also, these results enable one to estimate when natural convection may create errors in membrane testing systems.

The analysis and results are of practical interest in reverse osmosis and other membrane separation processes. The more productive the system, the more likely it will be that buoyancy effects are important.

In liquid-phase membrane separation processes, one is interested in understanding the fundamental transport processes occurring within the membrane structure and in studying the nonlinear diffusional effects on the feed solution side of the membrane. In particular, the phenomenon of polarization or accumulation of the rejected component at the membrane surface is significant since it limits the efficiency of such a process. Several papers, mostly of a theoretical nature have appeared in the literature, which have investigated methods of predicting the extent of polarization with various geometries under laminar and turbulent flow conditions (*3, 9* to *11, 20, 22*). It has been found that polarization can be a very important factor in the design of practical equipment.

The high degree of polarization found in laminar flows implies large concentration gradients and therefore significant buoyancy effects. Under low flow rates therefore, natural convection may be quite significant, as has been exemplified by the results of heat transfer calculations (*4* to *6, 8, 12, 17* to *19*). The analysis of heat transfer systems is much simpler than the corresponding reverse osmosis problem because of the boundary conditions involved. It has been shown by dispersion experiments (*15, 16*), that very small differences in density can cause significant variations in the velocity profile. Furthermore, some of the experimental results of Merten, et al. (*13*) did not agree very well with the theoretical prediction of the water flux by Srinivasan, et al. (*22*) at low flow rates. On an intuitive basis, Srinivasan, et al. pointed out that this apparent discrepancy could be at least partially explained on the basis of natural convection effects, due to the high Grashof numbers characteristic of the experiments involved. For sea water $N_{Gr} \simeq 6{,}000$ and for brackish water $N_{Gr} \simeq 800$.

The present analysis is aimed at:

1. Finding a suitable method of analysis which enables one to solve the transport equations for vertical flows with the boundary conditions which describe reverse osmosis and other mass transfer processes.
2. Investigating the effect of natural convection on polarization which is very important in reverse osmosis systems.
3. Determining the effect of buoyancy on Sherwood numbers with wall flux as a parameter.
4. Studying hydrodynamic instabilities created by buoyancy effects and to determine critical values of the buoyancy parameters.

ANALYSIS

Figure 1 gives a schematic description of the problem under investigation. Brine solution under pressure is forced into a vertical flat duct, the walls of which are made of a semipermeable membrane. The vertical configuration was chosen purposely because it is two dimensional. In a horizontal system unsymmetrical circulation effects make the system three dimensional and the analysis of such systems is extremely complicated.

The region of interest is far downstream from the inlet, where the concentration and velocity profiles are fully developed. Here the concentration polarization is greatest as are the buoyancy effects. Thus in effect, the resulting solution of the problem will be an asymptotic one.

Brine is assumed to enter the duct with a fully developed velocity profile and at the bulk velocity U_{b0}. The distance between the walls is $2h$ and the interfacial velocity is $v_w{}^+$ which is assumed to be very small compared to U_{b0}. It will be assumed that $v_w{}^+$ is constant along the axis. Gravitational components are g_x and g_y. For the vertical system $g_x = +g$; $g_y = 0$. The coordinate system is depicted in Figure 1.

To facilitate the analysis, it will be assumed that the flow is laminar, steady, fully developed and two dimensional. All physical properties are constant, except for variation of density in the buoyancy term.

The continuity equation is

$$\frac{\partial w}{\partial \xi} + \frac{\partial v}{\partial \eta} = 0 \tag{1}$$

and the equations of motion are:

x component

$$w\frac{\partial w}{\partial \xi} + v\frac{\partial w}{\partial \eta} = -\frac{\partial p}{\partial \xi} + \frac{1}{N_{Re}}\left[\frac{\partial^2 w}{\partial \xi^2} + \frac{\partial^2 w}{\partial \eta^2}\right]$$

$$-\frac{1}{N_{Fr}} - \frac{N_{Gr}}{N_{Re}{}^2}(\theta - 1) \tag{2}$$

where the density variation is given by the equation of state

$$\frac{\rho}{\rho_0} = 1 - \beta\,(c_s - c_{s0}) \tag{2a}$$

y component

$$w\frac{\partial v}{\partial \xi} + v\frac{\partial v}{\partial \eta} = -\frac{\partial p}{\partial \eta} + \frac{1}{N_{Re}}\left[\frac{\partial^2 v}{\partial \xi^2} + \frac{\partial^2 v}{\partial \eta^2}\right] \tag{3}$$

and neglecting axial diffusion, the convective diffusion equation is

$$w\frac{\partial \theta}{\partial \xi} + v\frac{\partial \theta}{\partial \eta} = \frac{1}{N_{Pe}}\frac{\partial^2 \theta}{\partial \eta^2} \tag{4}$$

The boundary conditions associated with the problem are:

1. No slip condition

$$w(1, \xi) = 0 \tag{5}$$

2. The interfacial velocity, $v_w{}^+$, is related to the driving force by the phenomenological law

$$v_w{}^+ = A[\Delta P - (\pi_w - \pi_p)] \tag{6}$$

π refers to the osmotic pressure which strictly is a function of concentration. To simplify the problem somewhat, we shall assume $\Delta P >> \pi_w$ so that

$$v_w{}^+ \simeq A \cdot \Delta P = \text{constant} \tag{7}$$

and we can write

$$v(1, \xi) = \frac{v_w{}^+}{U_{b0}} = v_w \tag{8}$$

3. Symmetry conditions at the center

$$\frac{\partial w}{\partial \eta}(0, \xi) = v(0, \xi) = 0 \tag{9}$$

For the diffusion equation we have:

1. Inlet condition

$$\theta(\eta, 0) = 1 \tag{10}$$

2. Symmetry condition

$$\frac{\partial \theta}{\partial \eta}(0, \xi) = 0 \tag{11}$$

3. A third boundary condition can be obtained by making a salt balance at the interface. Thus

$$N_s = \rho c_s v_w{}^+\big|_{y=h} - \rho D \frac{\partial c_s}{\partial y}\bigg|_{y=h}$$

(salt flux through the wall) (bulk flow term) (diffusion term)

or since for an ideal membrane there is no salt leakage through the wall, $N_s = 0$, which yields

$$\alpha \frac{\partial \theta}{\partial \eta}\bigg|_{\eta=1} = \theta\bigg|_{\eta=1} \tag{12}$$

where

$$\alpha = \frac{D}{v_w{}^+ h}$$

α is the reciprocal of the wall Peclet number. Therefore it reflects the intensity of mass transfer through the walls and is small for large mass transfer rates. α is to be distinguished from the reciprocal inlet Peclet number due to axial flow. The problem thus reduces to solving Equations (1) through

(4) with the boundary conditions (5) through (12).

Combined free and forced convection problems have been treated in the past in a variety of situations in heat transfer. Sparrow and Gregg (*21*) have obtained exact similarity solutions using a combination of variables for coupled forced and natural convection flows over a vertical flat plate. Subsequently, Carter and Gill (*6*) studied combined free and forced convection in porous conduits with flow through the walls and used a technique whereby the dependent variable was chosen so that the partial differential equations could be reduced to a set of total differential equations. However the boundary condition given by Equation (12) seems to have no exact analogue in heat transfer and these methods are inapplicable in the present study. A characteristic feature of all these problems is the intimate coupling of the momentum and the diffusion or energy equations which make them difficult to solve. Approximate methods are very often necessary to solve the two equations simultaneously.

Some simplification may be achieved by defining a stream function ψ such that

$$w = \frac{\partial \psi}{\partial \eta} \quad ; \quad v = -\frac{\partial \psi}{\partial \xi} \tag{13}$$

Further, Equations (3) and (2) may be differentiated with respect to ξ and η respectively, and subtracting the results, one can eliminate the pressure terms to obtain

$$\frac{\partial}{\partial \xi}\left[w\frac{\partial v}{\partial \xi}\right] + \frac{\partial}{\partial \xi}\left[v\frac{\partial v}{\partial \eta}\right] + \frac{1}{N_{Re}}\frac{\partial}{\partial \eta}\left[\frac{\partial^2 w}{\partial \xi^2} + \frac{\partial^2 w}{\partial \eta^2}\right] - \frac{\partial}{\partial \eta}\left[w\frac{\partial w}{\partial \xi}\right] - \frac{\partial}{\partial \eta}\left[v\frac{\partial w}{\partial \eta}\right] - \frac{N_{Gr}}{N_{Re}^2}\frac{\partial \theta}{\partial \eta} = \frac{1}{N_{Re}}\frac{\partial}{\partial \xi}\left[\frac{\partial^2 v}{\partial \xi^2} + \frac{\partial^2 v}{\partial \eta^2}\right] \tag{14}$$

which has to be solved together with the convective diffusion equation

$$v\frac{\partial \theta}{\partial \eta} + w\frac{\partial \theta}{\partial \xi} = \frac{1}{N_{Pe}}\frac{\partial^2 \theta}{\partial \eta^2} \tag{15}$$

using Equations (5) through (12).

It has been shown by Berman (*2*) that for a system with no buoyancy effects and a constant velocity at the interface, the stream function can be defined such that

$$\psi = (1 - B\xi)\ F(\eta) \tag{16}$$

where B is a constant which can be evaluated by a mass balance. For this problem B becomes equal to v_w. Thus in the absence of a body force term Equations (13), (14), and (16) would enable one to obtain a total differential equation in $F(\eta)$. However, due to the presence of the body force in this problem, it is necessary to define a more general stream function as

$$\psi = (1 - v_w\xi)\ F(\eta, \xi) \tag{17}$$

However this simplifies the problem significantly only if F is approximately a function of η only. That is, only if F is a weak function of ξ and this will be shown to be the case.

If F is a function of η only, then the following terms in Equation (14),

$$\frac{\partial}{\partial \xi}\left[w\frac{\partial v}{\partial \xi}\right], \frac{\partial}{\partial \xi}\left[v\frac{\partial v}{\partial \eta}\right], \frac{\partial}{\partial \eta}\left[\frac{\partial^2 w}{\partial \xi^2}\right], \frac{\partial}{\partial \xi}\left[\frac{\partial^2 v}{\partial \xi^2}\right]$$

and

$$\frac{\partial}{\partial \xi}\left[\frac{\partial^2 v}{\partial \eta^2}\right]$$

are identically zero. Since F depends only weakly on ξ, these terms are small and can be neglected as would be the case in boundary layer flows. Equation (14) then simplifies to

$$\frac{1}{N_{Re}}\frac{\partial}{\partial \eta}\left[\frac{\partial^2 w}{\partial \eta^2}\right] - \frac{\partial}{\partial \eta}\left[w\frac{\partial w}{\partial \xi}\right] - \frac{\partial}{\partial \eta}\left[v\frac{\partial w}{\partial \eta}\right] - \frac{N_{Gr}}{N_{Re}^2}\frac{\partial \theta}{\partial \eta} = 0 \tag{18}$$

This equation has to be solved simultaneously with Equation (15). The assumptions made to arrive at Equation (18) are essentially the same as those used by Prandtl when he presented his analysis on the external flow over slender bodies, that is elimination of Equation (3) and assumption that the pressure is constant in the boundary layer along the direction normal to the surface.

SOLUTION OF THE RESULTANT EQUATIONS

Several methods were tried in an attempt to solve this set of coupled equations. Details are given elsewhere (*14*). The method which was successful was a perturbation scheme which employed the buoyancy parameter N_{Gr}/N_{Re}^2 as the perturbation parameter. Thus one may define

$$F(\eta, \xi) = F_0(\eta) + \sum_{k=1}^{\infty} \epsilon^k\ F_k(\eta, \xi) \tag{19}$$

and

$$\theta(\eta, \xi) = \theta_0(\eta, \xi) + \sum_{k=1}^{\infty} \epsilon^k\ \theta_k(\eta, \xi) \tag{20}$$

where

$$\epsilon = \frac{N_{Gr}}{N_{Re}^2}$$

The zeroth-order function F_0 was chosen as a function of η only, so as to conform with the solution of the problem with no buoyancy. Equations (13) and (17) in conjunction with Equations (19) and (20) yield

$$w = (1 - v_w\xi)\left[F_0'(\eta) + \sum_{k=1}^{\infty} \epsilon^k \frac{\partial F_k}{\partial \eta}\right] \tag{21}$$

$$v = v_w\left[F_0 + \sum_{k=1}^{\infty} \epsilon^k\ F_k\right] - (1 - v_w\xi)\sum_{k=1}^{\infty} \epsilon^k \frac{\partial F_k}{\partial \xi} \tag{22}$$

By substituting Equations (20), (21), and (22) in the momentum and diffusion equations and equating coefficients of like powers of ϵ, one generates an infinite series of differential equations for the F_k and θ_k functions.

The zeroth-order equations do not include the term $N_{Gr}/N_{Re}^2\ (\partial\theta/\partial\eta)$ and they are given as

$$\frac{F_0^{1v}}{N_{Re}} + v_w\frac{d}{d\eta}[\{F_0'\}^2] - v_w\frac{d}{d\eta}[F_0\ F_0''] = 0 \tag{23}$$

and

$$(1 - v_w\xi)\ F_0'\frac{\partial \theta_0}{\partial \xi} + v_w F_0\frac{\partial \theta_0}{\partial \eta} = \frac{1}{N_{Pe}}\frac{\partial^2 \theta_0}{\partial \eta^2} \tag{24}$$

with the boundary conditions

$$F_0'(1) = F_0(0) = F_0''(0) = 0; \quad F_0(1) = 1 \tag{25}$$

$$\frac{\partial \theta_0}{\partial \eta}(0, \xi) = 0; \quad \theta_0(\eta, 0) = 1; \quad \alpha\frac{\partial \theta_0}{\partial \eta}(1, \xi) = \theta_0(1, \xi) \tag{26}$$

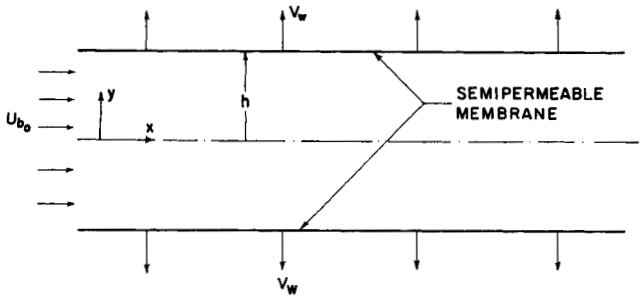

Fig. 1. Schematic diagram of the system.

Equations (23) through (26) are identical to the equations solved by previous investigators (*2, 9, 20*). Since v_w is small under the conditions which prevail in liquid phase membrane separation processes, one can expand $F_0(\eta)$ in a perturbation series about the wall Reynolds number. Thus letting

$$F_0(\eta) = F_{00}(\eta) + \sum_{m=1}^{\infty} N_{Re_w}{}^m \; F_{0m}(\eta) \qquad (27)$$

where

$$N_{Re_w} = v_w \; N_{Re} \qquad (27a)$$

it can be shown (*20*) that the first and higher order terms can be neglected for the small values of N_{Re_w} which are of interest in the reverse osmosis problem. For the zero order term one gets

$$F_{00}(\eta) = \frac{3\eta}{2} - \frac{\eta^3}{2} \qquad (28)$$

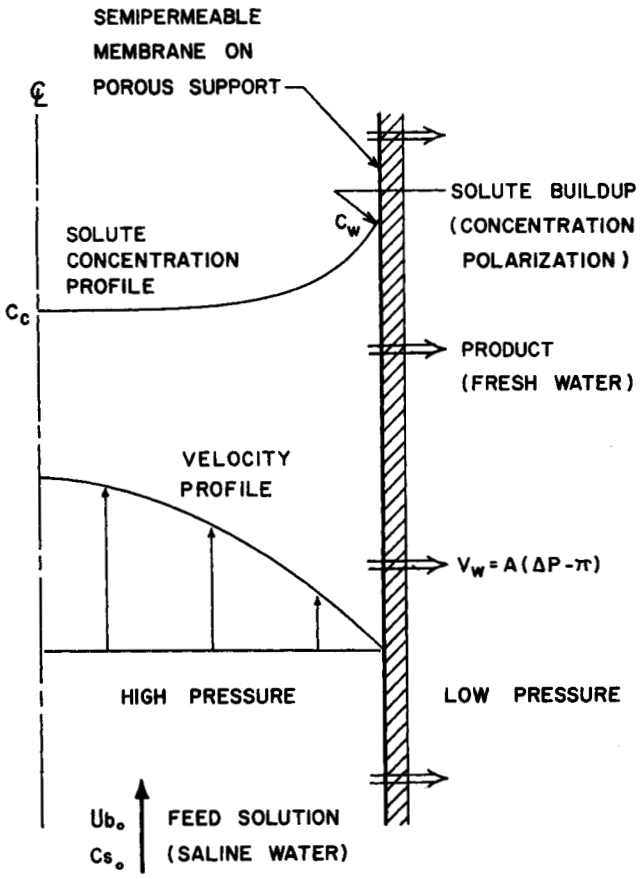

Fig. 1*a*. Schematic diagram of the system.

The concentration profile may be obtained by the method of separation of variables by letting

$$\theta_0 = \sum_{n=0}^{\infty} B_n \; Y_n(\eta) \quad [1 - v_w\xi]^{(2/3\;\beta_n - 1)} \qquad (29)$$

and the B_n, Y_n and β_n are known (*20*) for several values of the parameters. The first order functions F_1 and θ_1 are obtained from

$$\frac{1}{N_{Re}} \frac{\partial^4 F_1}{\partial \eta^4} - \frac{\partial}{\partial \eta}\Bigg[-2 \; v_w \; F_0' \frac{\partial F_1}{\partial \eta} + F_0' \frac{\partial^2 F_1}{\partial \xi \partial \eta} (1 - v_w\xi) + v_w F_1 F_0'' + v_w F_0 \frac{\partial^2 F_1}{\partial \eta^2} - F_0'' \; (1 - v_w\xi) \frac{\partial F_1}{\partial \xi} \Bigg] - \frac{1}{(1 - v_w\xi)} \frac{\partial \theta_0}{\partial \eta} = 0 \qquad (30)$$

and

$$\frac{\partial}{\partial \xi}\Bigg[(1 - v_w\xi) \left(\theta_0 \frac{\partial F_1}{\partial \eta} + F_0' \theta_1 \right) \Bigg] + \frac{\partial}{\partial \eta}\Bigg[\left\{ v_w F_1 - \frac{\partial F_1}{\partial \xi} (1 - v_w\xi) \right\} \theta_0 + v_w F_0 \theta_1 \Bigg] = \frac{1}{N_{Pe}} \frac{\partial^2 \theta_1}{\partial \eta^2} \qquad (31)$$

with the associated boundary conditions

$$\frac{\partial F_1}{\partial \eta}(1, \xi) = F_1(1, \xi) = \frac{\partial^2 F_1}{\partial \eta^2}(0, \xi) = F_1(0, \xi) = 0 \qquad (32)$$

$$\theta_1(\eta, 0) = \frac{\partial \theta_1}{\partial \eta}(0, \xi) = 0; \quad \alpha \frac{\partial \theta_1}{\partial \eta}(1, \xi) = \theta_1(1, \xi) \qquad (33)$$

The above system of Equations (30) to (33) is extremely difficult to solve exactly. Substitution of Equation (29) in Equation (30) yields

$$\frac{1}{N_{Re}} \frac{\partial^4 F_1}{\partial \eta^4} - \frac{\partial}{\partial \eta}\Bigg[-2 \; v_w \; F_0' \frac{\partial F_1}{\partial \eta} + F_0' \frac{\partial^2 F_1}{\partial \xi \partial \eta} (1 - v_w\xi) + v_w F_1 F_0'' + v_w F_0 \frac{\partial^2 F_1}{\partial \eta^2} - F_0'' \; (1 - v_w\xi) \frac{\partial F_1}{\partial \xi} \Bigg] - \frac{1}{(1 - v_w\xi)} \sum_{n=0}^{\infty} B_n Y_n' \; (1 - v_w\xi)^{(2/3\;\beta_n - 1)} = 0 \qquad (34)$$

The key to solving Equation (34) can be found by careful inspection which reveals that the transformation

$$F_1(\eta, \xi) = N_{Re} \sum_{j=1}^{\infty} \phi_j(\eta) \; (1 - v_w\xi)^{(2/3\;\beta_{j-1} - 2)} = 0 \qquad (35)$$

reduces this partial differential equation to a system of total differential equations in the ϕ_j functions. Further, this transformation is consistent with all of the boundary conditions. In addition, the dependency of F_1 on ξ arises only as the product $v_w\xi$ and since v_w is small in the applications considered here, F_1 is indeed a weak function of ξ. It is easy to show that the ϕ_j function must satisfy the equation

$$\phi_j{}^{iv} - N_{Re_w} \frac{d}{d\eta}\Bigg[F_0 \phi_j'' - \frac{2}{3} \beta_{j-1} \; F_0' \phi_j' + \left(\frac{2}{3} \beta_{j-1} - 1 \right) F_0'' \phi_j \Bigg] - B_{j-1} \; Y'_{j-1} = 0 \qquad (36)$$

with the associated boundary conditions

$$\phi_j(0) = \phi_j''(0) = \phi_j'(1) = \phi_j(1) = 0 \qquad (37)$$

Equations (36) and (37) may be solved exactly but if we are interested mainly in processes which involve small values of v_w, as is the case of reverse osmosis, then it is both very accurate and very much simpler to follow the same procedure adopted before and define

$$\phi_j(\eta) = \phi_{j0} + \sum_{m=1}^{\infty} N_{Rew}{}^m \phi_{jm}(\eta) \qquad (38)$$

The equation associated with ϕ_{j0} is

$$\phi_{j0}{}^{iv} - B_{j-1} Y'_{j-1} = 0 \qquad (39)$$

$$\phi_{j0}(0) = \phi_{j0}''(0) = \phi_{j0}'(1) = \phi_{j0}(1) = 0 \qquad (40)$$

The solution of this equation is readily seen to be

$$\phi_{j0} = B_{j-1} \int_0^{\eta} \int_0^{w} \int_0^{\tau} Y_{j-1}\, d\eta d\tau dw + \frac{A_{j0}\eta^3}{6} + \frac{B_{j0}\eta^2}{2} + C_{j0}\eta + D_{j0} \qquad (41)$$

From Equation (40) it is easy to show that

$$B_{j0} = D_{j0} = 0 \qquad (42)$$

and

$$A_{j0} = 3B_{j-1}\left[\int_0^1 L_2(\eta)\, d\eta - \int_0^1 L_1(\eta)\, d\eta \right] \qquad (43a)$$

$$C_{j0} = \frac{B_{j-1}}{2} \int_0^1 L_1(\eta)\, d\eta - \frac{3B_{j-1}}{2} \int_0^1 L_2(\eta)\, d\eta \qquad (43b)$$

where

$$L_1(\eta) = \int_0^{\eta} Y_{j-1}(\eta)\, d\eta \qquad (43c)$$

and

$$L_2(\eta) = \int_0^{\eta} \int_0^{\tau} Y_{j-1}(\eta)\, d\eta d\tau \qquad (43d)$$

and from reference *20*

$$B_{j-1} = \frac{\int_0^1 \frac{(1-\eta^2)}{\alpha} \exp\left[\frac{\eta^2(\eta^2-6)}{8\alpha} \right] Y_{j-1}(\eta)\, d\eta}{\int_0^1 \frac{(1-\eta^2)}{\alpha} \exp\left[\frac{\eta^2(\eta^2-6)}{8\alpha} \right] Y_{j-1}^2(\eta)\, d\eta} \qquad (43e)$$

The series in Equation (35) is rapidly converging since the eigenvalues increase rapidly. Hence only the first- and second-order terms need be taken into account.

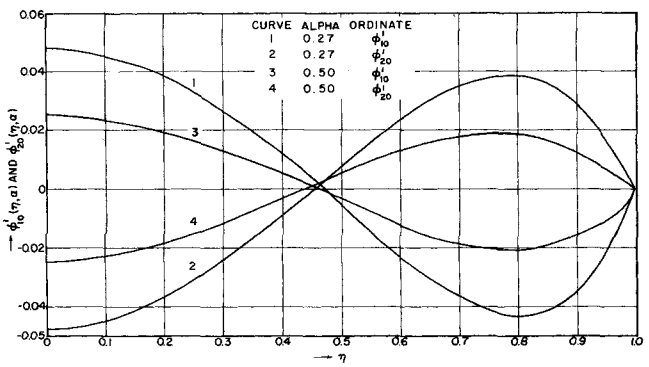

Fig. 2. The function of ϕ_{10}' and ϕ_{20}' for $\alpha = 0.5$ and $\alpha = 0.27$.

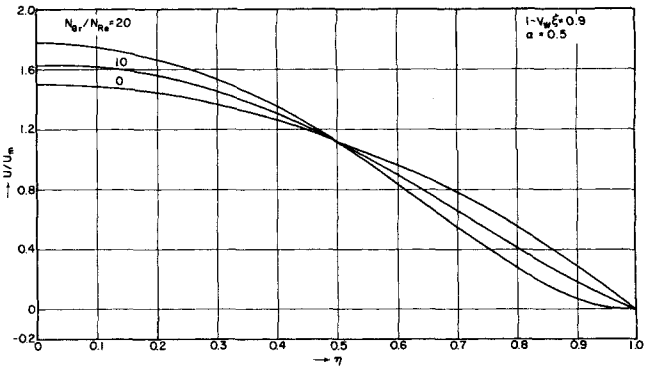

Fig. 2a. Axial velocity profiles for various N_{Gr}/N_{Re} ratios in upward flow.

The next problem is to determine θ_1. By using Equations (28), (29) and (35), Equation (31) can be simplified to

$$F_{00}' \frac{\partial\theta_1}{\partial\xi}(1-v_w\xi) + v_w F_{00} \frac{\partial\theta_1}{\partial\eta} = \frac{1}{N_{Pe}} \frac{\partial^2\theta_1}{\partial\eta^2} + Q(\xi,\eta) \qquad (44)$$

where

$$Q(\xi,\eta) = -\frac{\partial}{\partial\xi}\left[(1-v_w\xi)\frac{\partial F_1}{\partial\eta}\theta_0 \right] - \frac{\partial}{\partial\eta}\left[\left\{ v_w F_1 - \frac{\partial F_1}{\partial\xi}(1-v_w\xi) \right\}\theta_0 \right] \qquad (44a)$$

Since

$$F_1 = N_{Re}\left[\frac{\phi_{10}}{(1-v_w\xi)^2} + \frac{\phi_{20}}{(1-v_w\xi)^{(2-2/3\,\beta_1)}} \right] \qquad (44b)$$

and

$$\theta_0 = \sum_{j=1}^{\infty} B_{j-1} Y_{j-1} (1-v_w\xi)^{(2/3\,\beta_{j-1}-1)} \qquad (44c)$$

one obtains

$$Q(\xi,\eta) = -N_{Re}\frac{\partial}{\partial\xi}\left[\left\{ \frac{\phi_{10}'}{(1-v_w\xi)} + \frac{\phi_{20}'}{(1-v_w\xi)^{1-2/3\,\beta_1}} \right\} \sum_{j=1}^{\infty} B_{j-1} Y_{j-1} (1-v_w\xi)^{(2/3\,\beta_{j-1}-1)} \right] + N_{Rew}\frac{\partial}{\partial\eta}\left[\left\{ \frac{\phi_{10}}{(1-v_w\xi)^2} + \frac{(1-2/3\,\beta_1)\phi_{20}}{(1-v_w\xi)^{2-2/3\,\beta_1}} \right\} \sum_{j=1}^{\infty} B_{j-1} Y_{j-1}(1-v_w\xi)^{(2/3\,\beta_{j-1}-1)} \right] \qquad (44d)$$

The inhomogeneity $Q(\xi,\eta)$ is difficult to handle in this form. However, some reasonably good assumptions may be made to simplify the problem. Thus it is known from heat transfer results that the effect of buoyancy is felt primarily on the velocity profiles and the effect on temperature profiles is relatively small. Similarly we can expect the concentration profile to be less affected by buoyancy than the velocity profiles and for evaluation of θ_1 it seems reasonable to approximate

$$\theta_0 \simeq \frac{B_0 Y_0}{1 - v_w\xi}$$

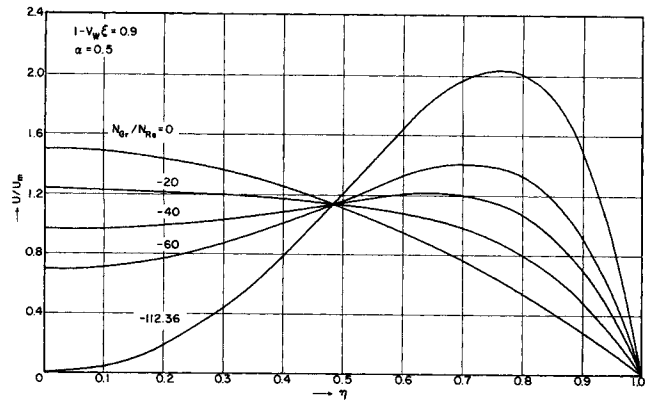

Fig. 3. Axial velocity profiles for various N_{Gr}/N_{Re} ratios in downward flow.

and hence

$$F_1 = \frac{N_{Re}\,\phi_{10}}{(1-v_w\xi)^2}$$

so that we obtain

$$Q(\xi,\eta) = \frac{B_0\,N_{Rew}}{(1-v_w\xi)^3}\,[Y_0'\,\phi_{10} - Y_0\,\phi_{10}'] \qquad (45)$$

The boundary conditions on θ_1 are

$$\frac{\partial\theta_1}{\partial\eta}(0,\xi) = \theta_1(\eta,0) = 0; \quad \alpha\frac{\partial\theta_1}{\partial\eta}(1,\xi) = \theta_1(1,\xi) \qquad (46)$$

Equation (44) may be put in a more convenient form by defining a new variable

$$\sigma = \frac{1}{N_{Pe}}\int_0^\xi \frac{d\xi}{(1-v_w\xi)} \qquad (47)$$

which transforms it to

$$F_{00}'\frac{\partial\theta_1}{\partial\sigma} + v_w\,F_{00}\frac{\partial\theta_1}{\partial\eta} = \frac{1}{N_{Pe}}\frac{\partial^2\theta_1}{\partial\eta^2} + Q(\sigma,\eta) \qquad (48)$$

Because of the function $Q(\sigma,\eta)$, Equation (48) can be solved most easily by applying the Duhamel theorem (*1*). One may define a new variable E, such that

$$F_{00}'\frac{\partial E}{\partial\sigma} + v_w\,F_{00}\frac{\partial E}{\partial\eta} = \frac{1}{N_{Pe}}\frac{\partial^2 E}{\partial\eta^2} + Q(\lambda,\eta) \qquad (49)$$

with

$$E(\lambda,\eta,0) = \frac{\partial E}{\partial\eta}(\lambda,0,\sigma) = 0 \qquad (49a)$$

$$\alpha\frac{\partial E}{\partial\eta}(\lambda,1,\sigma) = E(\lambda,1,\sigma) \qquad (49b)$$

where λ is a constant. The solution for θ is then obtained by using the Duhamel integral as

$$\theta_1(\sigma,\eta) = \frac{\partial}{\partial\sigma}\int_0^\sigma E(\lambda,\eta,\sigma-\lambda)\,d\lambda \qquad (50)$$

Now, let

$$E(\lambda,\eta,\sigma) = E_1(\lambda,\eta) + E_2(\lambda,\eta,\sigma) \qquad (51)$$

and we obtain

$$\frac{F_{00}}{\alpha}\frac{dE_1}{d\eta} = \frac{d^2E_1}{d\eta^2} + Q_1(\lambda,\eta) \qquad (52)$$

with the conditions

$$\frac{dE_1}{d\eta}(\lambda,0) = 0 \qquad (52a)$$

$$\frac{dE_1}{d\eta}(\lambda,1) = \frac{1}{\alpha}E_1(\lambda,1) \qquad (52b)$$

where

$$Q_1(\lambda,\eta) = \frac{B_0}{\alpha}\,e^{\frac{3\lambda}{\alpha}}\,[Y_0'\,\phi_{10} - Y_0\,\phi_{10}'] \qquad (52c)$$

The solution of Equation (52) can be readily evaluated as

$$E_1(\lambda,\eta) = \int_0^\eta G_1(\eta,\lambda)\,d\eta - \int_0^1 G_1(\eta,\lambda)\,d\eta + \alpha G_1(1,\lambda) \qquad (53)$$

where

$$G_1(\eta,\lambda) = \frac{-\int_0^\eta \exp\left[-\frac{1}{\alpha}\left(\frac{3\eta^2}{4}-\frac{\eta^4}{8}\right)\right]Q_1(\lambda,\eta)\,d\eta}{\exp\left[-\frac{1}{\alpha}\left(\frac{3\eta^2}{4}-\frac{\eta^4}{8}\right)\right]} \qquad (53a)$$

The differential equation associated with E_2 is

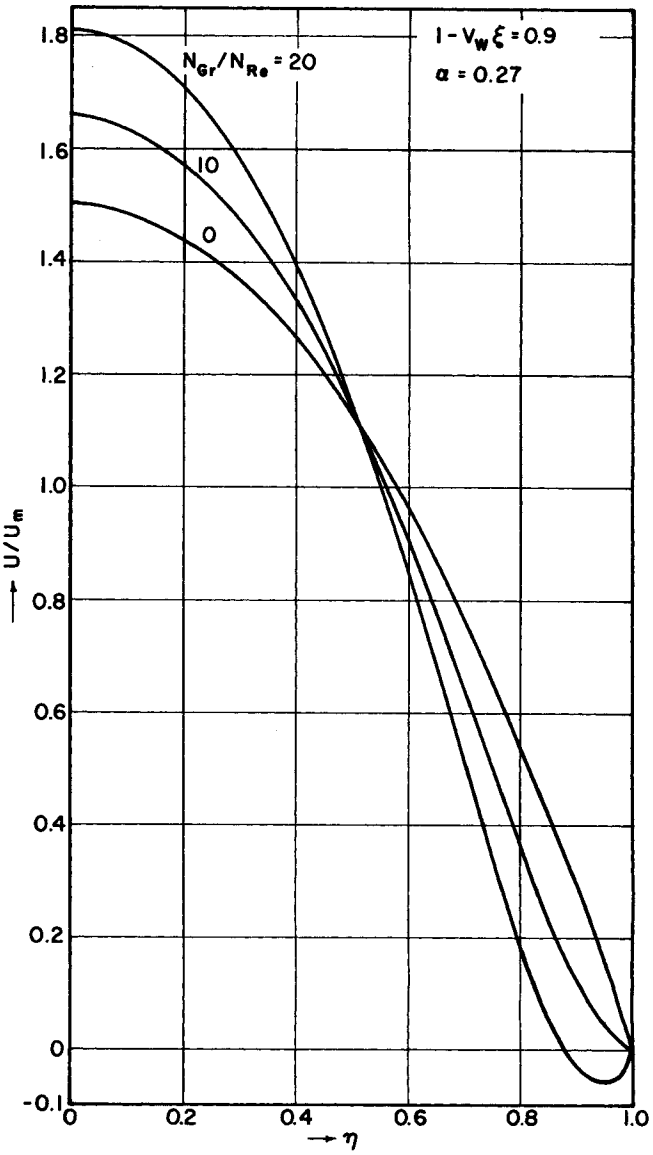

Fig. 4. Axial velocity profiles for various N_{Gr}/N_{Re} ratios in upward flow.

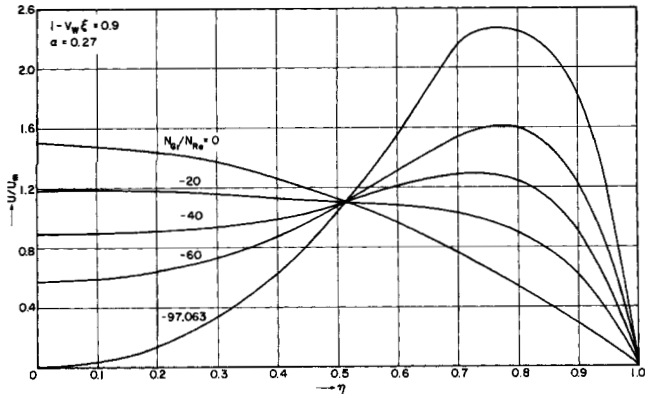

Fig. 5. Axial velocity profiles for various N_{Gr}/N_{Re} ratios in downward flow.

$$F_{00}'\frac{\partial E_2}{\partial \sigma}+\frac{F_{00}}{\alpha}\frac{\partial E_2}{\partial \eta}=\frac{\partial^2 E_2}{\partial \eta^2} \tag{54}$$

with the boundary conditions

$$E_2(0,\lambda,\eta)=-E_1(\lambda,\eta) \tag{54a}$$

$$\frac{\partial E_2}{\partial \eta}(\sigma,\lambda,0)=0 \tag{54b}$$

$$\frac{\partial E_2}{\partial \eta}(\sigma,\lambda,1)=\frac{1}{\alpha}E_2(\sigma,\lambda,1) \tag{54c}$$

By separation of variables, the solution is seen to be identical to that for θ_0 with the only difference being the expansion coefficients. Hence we may write

$$E_2(\sigma,\lambda,\eta)=\sum_{n=0}^{\infty}c_n(\lambda)\,Y_n(\eta)\chi_n(\sigma) \tag{55}$$

where

$$c_n(\lambda)=-\frac{\int_0^1 E_1(\lambda,\eta)\,\rho(\eta)\,Y_n(\eta)\,d\eta}{\int_0^1 \rho(\eta)\,Y_n^2(\eta)\,d\eta} \tag{55a}$$

and $\rho(\eta)$ is the weighting function given by

$$\rho(\eta)=\frac{(1-\eta^2)}{\alpha}\exp\left[\frac{\eta^2(\eta^2-6)}{8\alpha}\right] \tag{55b}$$

The $Y_n(\eta)$ correspond to the same eigenfunctions as before. Substituting the functions E_1 and E_2 in Equation (50), one obtains

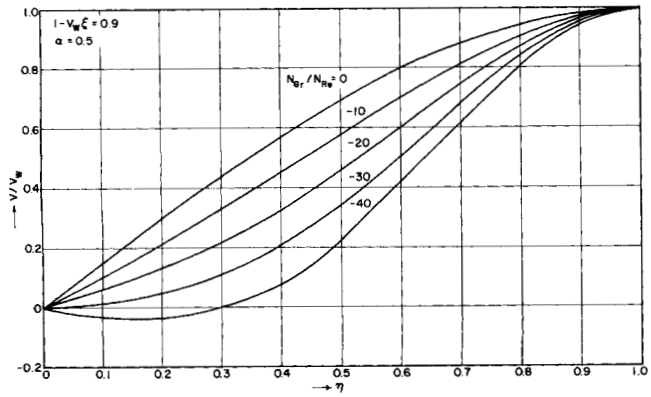

Fig. 6. Radial velocity profiles for various N_{Gr}/N_{Re} ratios in downward flow.

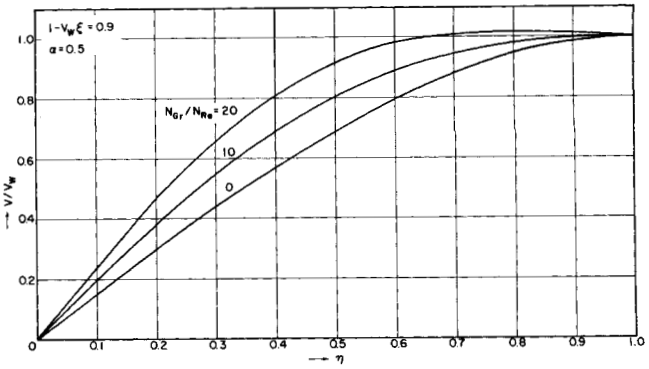

Fig. 7. Radial velocity profiles for various N_{Gr}/N_{Re} ratios in upward flow.

$$\theta_1(\xi,\eta)=\frac{H(\eta)}{(1-v_w\xi)^3}-\sum_{n=0}^{\infty}\frac{D_n\,Y_n(\eta)}{\left[\frac{2}{3}\beta_n+2\right]}\left\{\frac{3}{(1-v_w\xi)^3}+(1-v_w\xi)^{(2/3\,\beta_n-1)}\left(\frac{2}{3}\beta_n-1\right)\right\} \tag{56}$$

where

$$H(\eta)=\frac{E_1(\lambda,\eta)}{e^{\frac{3\lambda}{\alpha}}} \tag{56a}$$

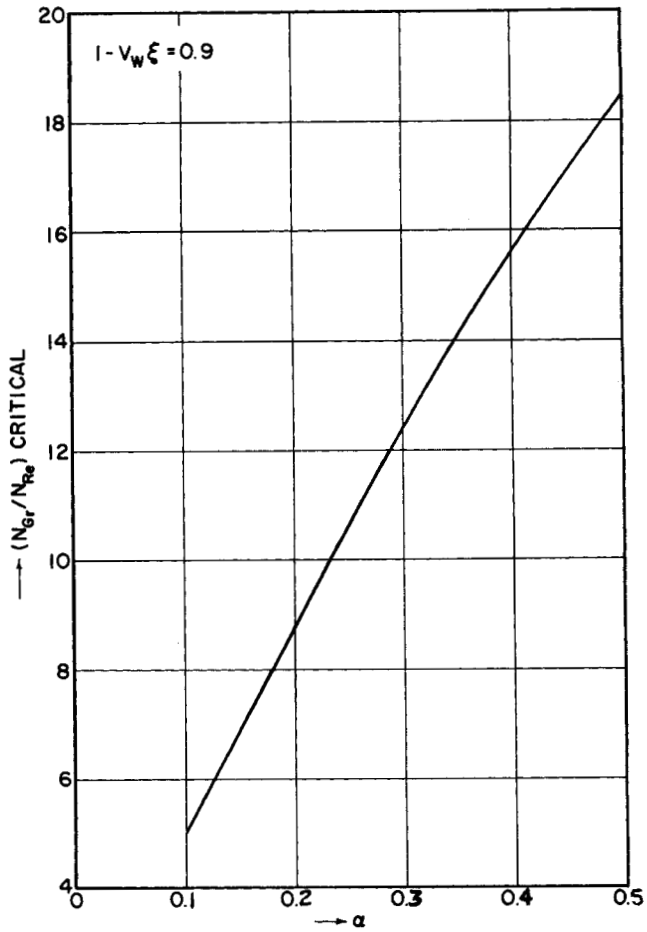

Fig. 8. Critical N_{Gr}/N_{Re} ratios in upward flows.

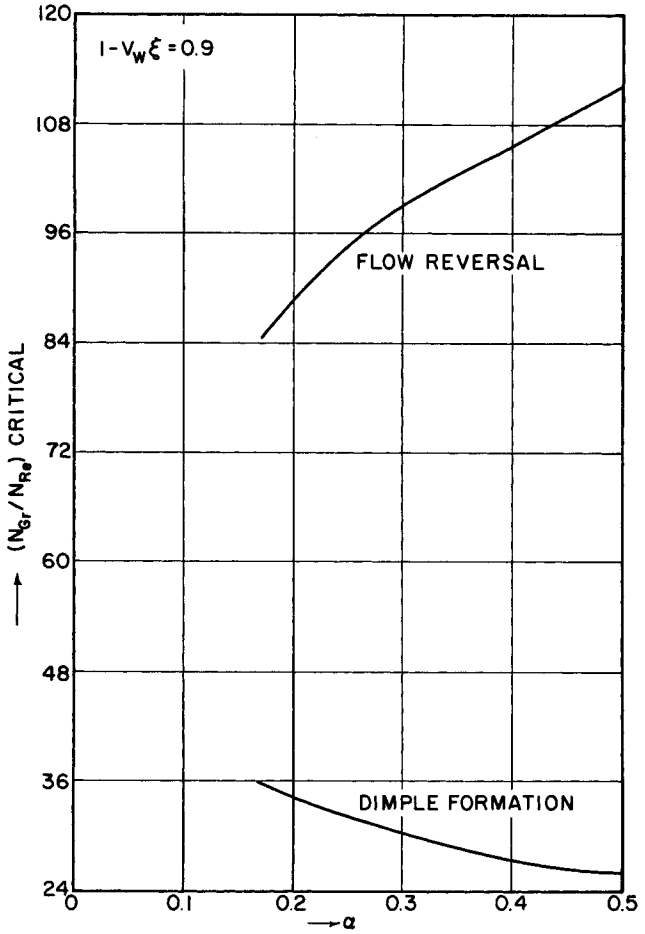

Fig. 9. Critical N_{Gr}/N_{Re} ratios in downward flow.

and

$$D_n = \frac{\int_0^1 H(\eta)\,\rho(\eta)\,Y_n(\eta)\,d\eta}{\int_0^1 \rho(\eta)\,Y_n^2(\eta)\,d\eta} \qquad (56b)$$

Determination of the second and higher order functions is very tedious because of the complexity of the equations.

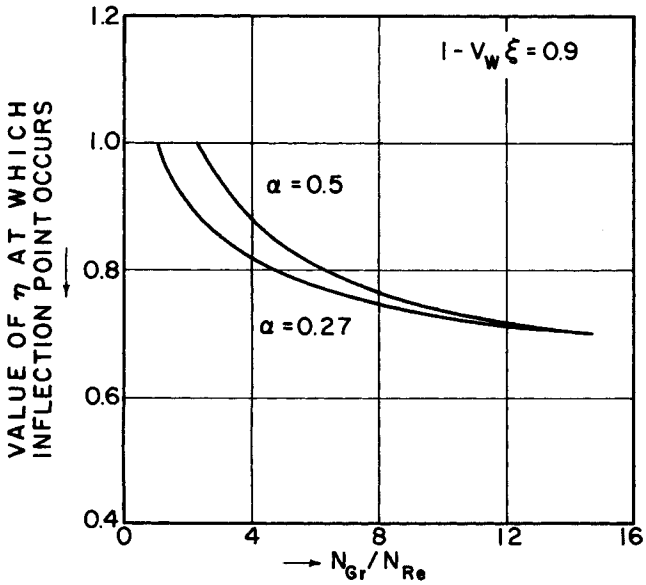

Fig. 10. Inflection point in upward flow denoted in Equation (63).

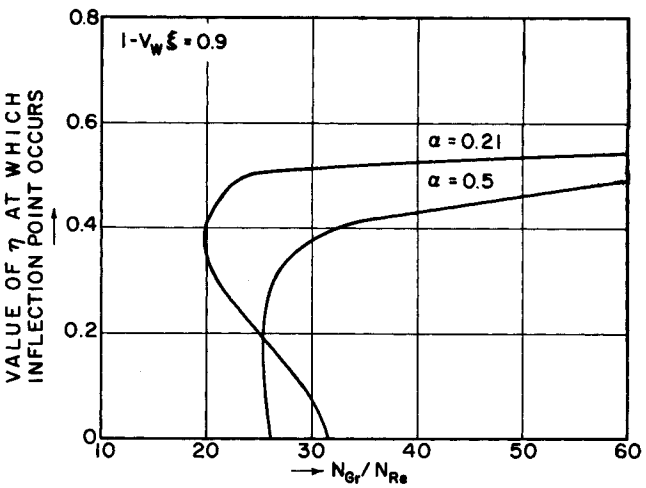

Fig. 11. Inflection points in downward flow denoted in Equation (63).

However, it would be expected that the contribution due to these terms is small over the range of parameters studied here. We shall therefore neglect second and higher order terms.

RESULTS AND DISCUSSION

The results of the above analysis may be summarized as

$$w = (1 - v_w\xi)\left[F_{00}' + \epsilon\frac{\partial F_1}{\partial \eta}\right] \qquad (57)$$

which may be rewritten in a more convenient form using Equations (28), (35), and (41) as

$$\frac{w}{w_{\text{Bulk}}} \simeq \frac{3}{2}(1-\eta^2) + \frac{N_{Gr}}{N_{Re}}\left[\frac{\phi_{10}'(\eta,\alpha)}{(1-v_w\xi)^2} + \frac{\phi_{20}'(\eta,\alpha)}{(1-v_w\xi)^{(2-2/3\,\beta_1)}}\right] \qquad (58)$$

where w_{Bulk} is $(1 - v_w\xi)$ and $\phi_{10}'(\eta, \alpha)$ and $\phi_{20}'(\eta, \alpha)$ are obtained from Equations (41), (42), and (43). The parametric dependence of w is given by

$$w = w\left(\xi, \eta, \frac{N_{Gr}}{N_{Re}^2}, N_{Re}, v_w, \alpha\right) \qquad (58a)$$

For arbitrarily large values of v_w, it is seen that the velocity distribution depends on two space variables ξ and η as well as the four parameters N_{Gr}/N_{Re}^2, v_w, N_{Re} and α. However, when one limits the discussion to small values of v_w, then the problem is markedly simplified to determining ϕ_{10} and ϕ_{20} which depend on η and α only. From Equations (22), (28), (35), and (41) it can be shown that

$$\frac{v}{v_w} = \frac{3\eta}{2} - \frac{\eta^3}{2} - \frac{N_{Gr}}{N_{Re}}\left[\frac{\phi_{10}(\eta,\alpha)}{(1-v_w\xi)^2} + \left(\frac{2}{3}\beta_1 - 1\right)\frac{\phi_{20}(\eta,\alpha)}{(1-v_w\xi)^{(2-2/3\,\beta_1)}}\right] \qquad (58b)$$

The concentration distribution also depends on two space variables and four parameters and this may be denoted as

$$\theta = \theta\left(\xi, \eta, \frac{N_{Gr}}{N_{Re}^2}, N_{Re}, v_w, \alpha\right) \qquad (59)$$

Using the perturbation method the concentration profile may be written as

$$\theta = \theta_0(\xi, \eta, N_{Re}, v_w, \alpha) + \frac{N_{Gr}}{N_{Re}^2}\theta_1(\xi, \eta, N_{Re}, v_w, \alpha) \tag{60}$$

and the expressions obtained in Equations (56) and (29) indicate that the quantities v_w and ξ occur only as the product $v_w\xi$ which physically represents the fraction of water removed. It should be noted that in momentum transfer, the parameter N_{Gr}/N_{Re} arises from Equation (58) and in the mass transfer equations the parameters N_{Gr}/N_{Re}^2 and N_{Re} have to be specified.

It is more useful to report concentration profiles in terms of the θ_w/θ_B ratio which is a measure of polarization at the membrane surface. The bulk concentration is obtained as

$$\theta_B = \frac{\int_0^1 \theta w d\eta}{\int_0^1 w d\eta} \tag{61}$$

The ratio of the wall to bulk concentration may be represented as

$$\frac{\theta_w}{\theta_B} = f\left(v_w\xi, \frac{N_{Gr}}{N_{Re}^2}, N_{Re}, \alpha\right) \tag{62}$$

Consequently if α and $v_w\xi$ are fixed, one can obtain the variation of polarization with the N_{Gr}/N_{Re}^2 ratio using N_{Re} as a parameter.

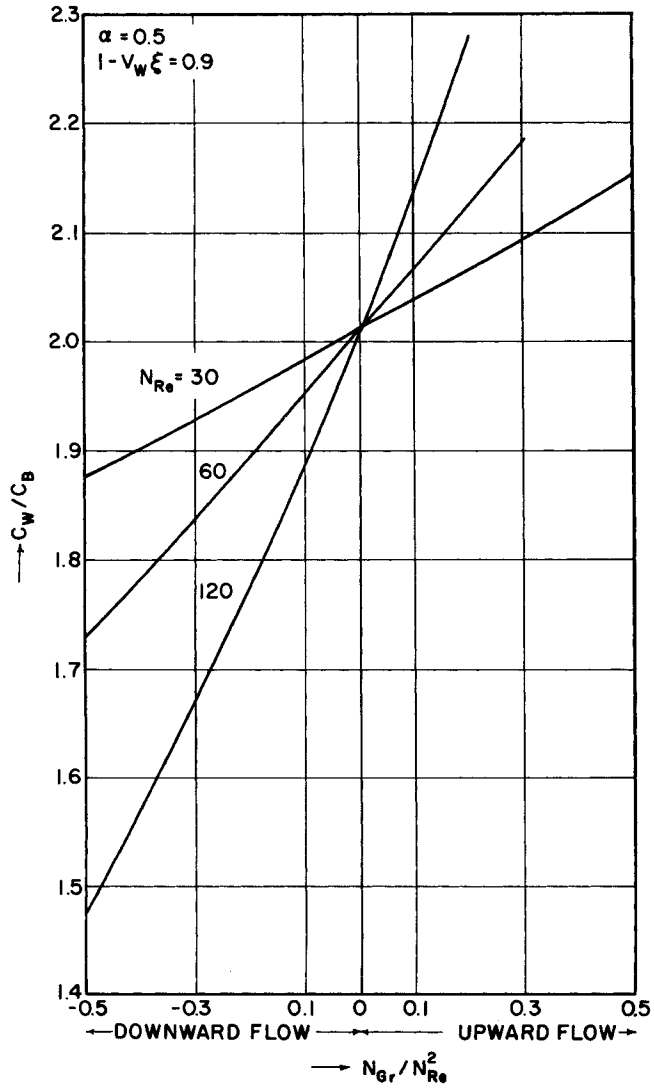

Fig. 12. Effect of buoyancy on polarization for different N_{Re}.

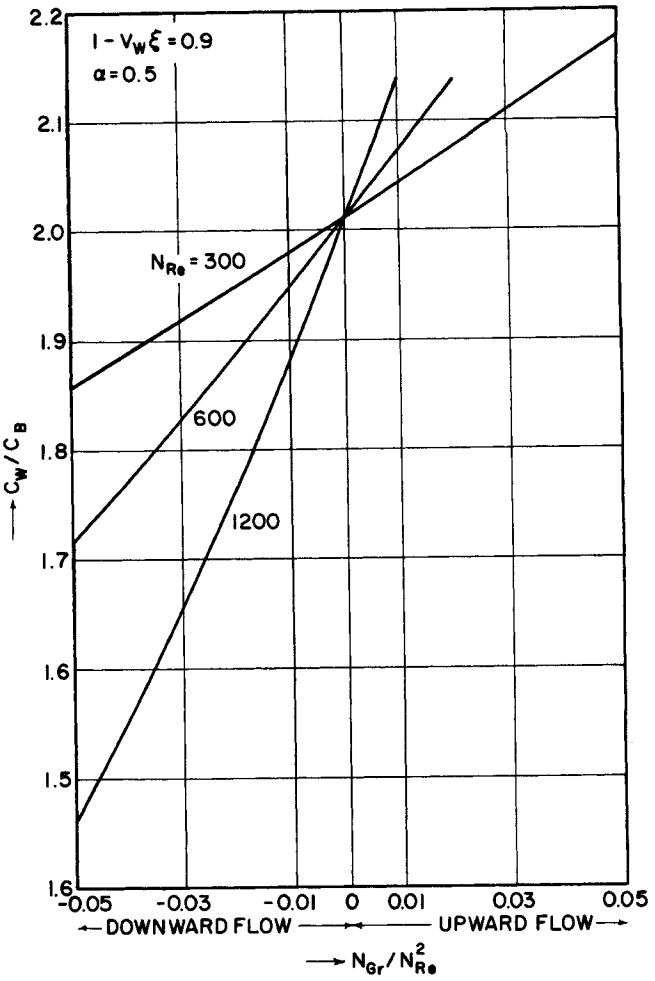

Fig. 12a. Effect of buoyancy on polarization at high N_{Re}.

All the integrals which had to be evaluated were determined numerically using Simpson's rule. The numerical calculations were performed for the values of the parameters

$$0.27 \leq \alpha \leq 0.5$$

$$30 \leq N_{Re} \leq 1200$$

$$-0.5 \leq \frac{N_{Gr}}{N_{Re}^2} \leq 0.5$$

$$0 \leq v_w\xi \leq 0.4$$

For the sake of brevity however, values will be reported only for $v_w\xi = 0.1$, since for other values of $v_w\xi$ the trend of the curves is the same.

It is of interest to consider this problem from two points of view. First, one is interested in the quantitative prediction of the effect of natural convection on mass transfer rates and the degree of polarization obtained in the system when the flow remains laminar. Secondly, the stability of the system is important. That is, it is of interest to know when the system will tend to become unstable hydrodynamically and will tend to become turbulent. This is of practical interest since turbulence markedly increases transverse mixing and thereby reduces polarization substantially. Thus, the results of the above analysis will be discussed from two points of view which are related to the:

1. Velocity profile distortion and related effects that pertain to the hydrodynamic stability of the system.
2. Effect of natural convection on polarization and mass transfer rates as reflected in the Sherwood numbers.

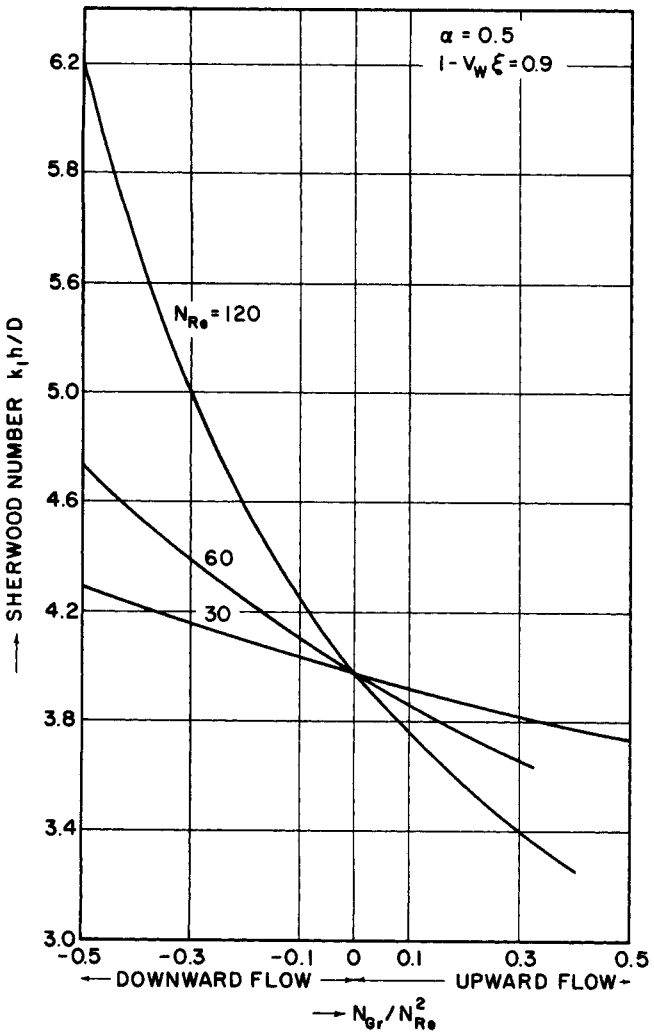

Fig. 13. Effect of buoyancy on Sherwood number at different N_{Re}.

Figure 2 indicates the behavior of the function ϕ_{10}' plotted against η with α as a parameter. According to Equation (58) only $\phi_{10}'(\alpha, \eta)$ and $\phi_{20}'(\alpha, \eta)$ need to be determined to find the effect of buoyancy on the velocity profile.

To give a better physical picture, by showing the complete velocity profile, Figure 2*a* illustrates the distortions in the velocity profile in upward flow due to natural convection for $\alpha = 0.5$. This is analogous to the heat transfer problem with cooling in upflow or heating in downflow. The results can be easily interpreted as follows. As concentration polarization becomes significant, the fluid particles closer to the wall are associated with a higher concentration and hence a greater density. On the other hand, at the center the concentration and density are lower. Hence there is a tendency for the fluid at the center to be subjected to an increased upward force due to buoyancy effects, and near the wall the reverse is true. The net effect is a distortion in the velocity profile, with an acceleration at the center and retardation near the walls. The magnitude of these distortions increases rapidly with buoyancy as is evident from Figure 2*a*. Ultimately as buoyancy effects increase, a situation is reached where the profile becomes flat at the wall since the velocity gradient goes to zero. This corresponds to the critical N_{Gr}/N_{Re} ratio. Beyond this value, the theory predicts a reversed flow near the wall. In actuality, however this would correspond to a hydrodynamically unstable system, with a tendency for separation near the wall. Analogous theoretical results have been obtained for heat transfer systems and experiments tend to confirm the theory (*12, 17*).

Results in Figure 3 illustrate the effect of buoyancy on downward flows. Here buoyancy opposes the flow and consequently one would expect a flattening of the velocity profile near the center and the gradient becomes steeper near the wall. Here a tendency toward instability occurs at the value of N_{Gr}/N_{Re} at which there is an incipient dimple like formation at the center of the flow. This inhibition of the velocity in the center of the duct has been observed experimentally for cooling in downflow or heating in upflow in heat transfer (*12, 17*).

Figures 4 and 5 illustrate the same trend shown in Figures 2*a* and 3 but the water flux is greater since $\alpha = 0.27$. One can see clearly, that the effect of increased flux is to increase buoyancy effects and thus the transition to an unstable flow occurs at a lower value of the N_{Gr}/N_{Re} ratio. This dependence on the parameter α has no counterpart in heat transfer and therefore is unique to mass transfer systems.

Figures 6 and 7 illustrate the effect of buoyancy on the radial velocity profiles for $\alpha = 0.5$. There is no significant effect other than increasing or decreasing the magnitude of v depending on the direction of flow.

From the axial velocity profiles, it is seen that natural convection can have a dominant role in causing the transi-

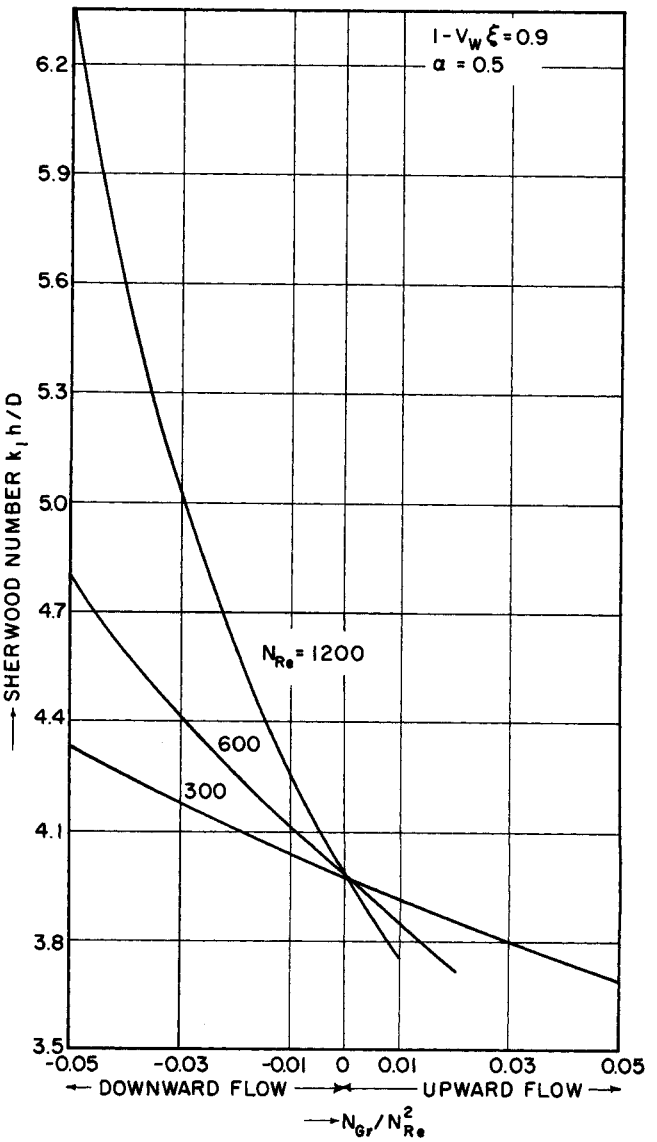

Fig. 13*a*. Effect of buoyancy on Sherwood number at high N_{Re}.

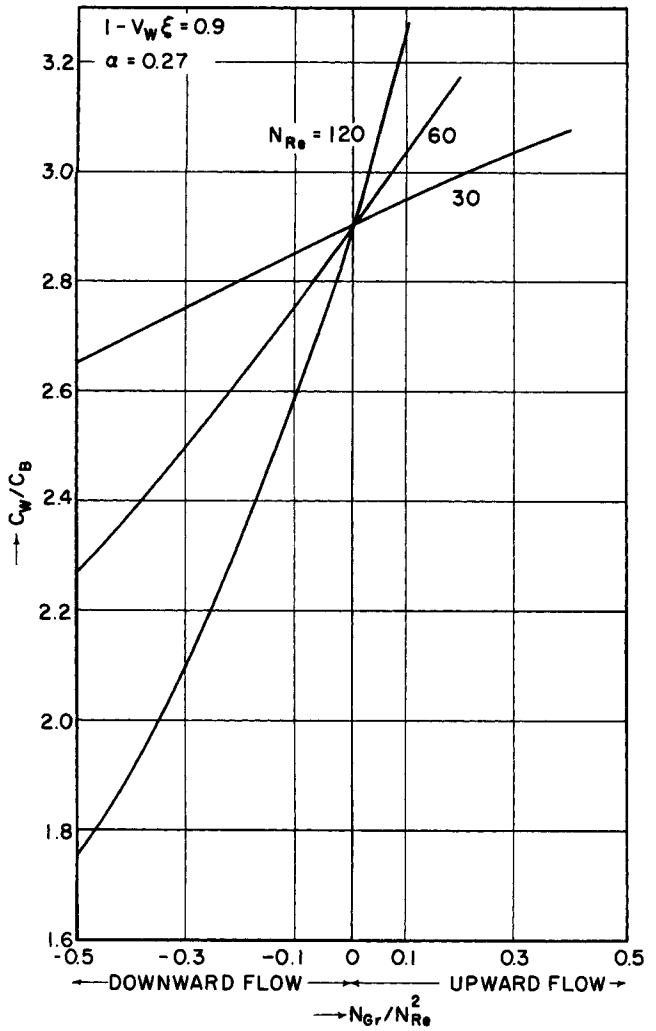

Fig. 14. Effect of buoyancy on polarization for different N_{Re}.

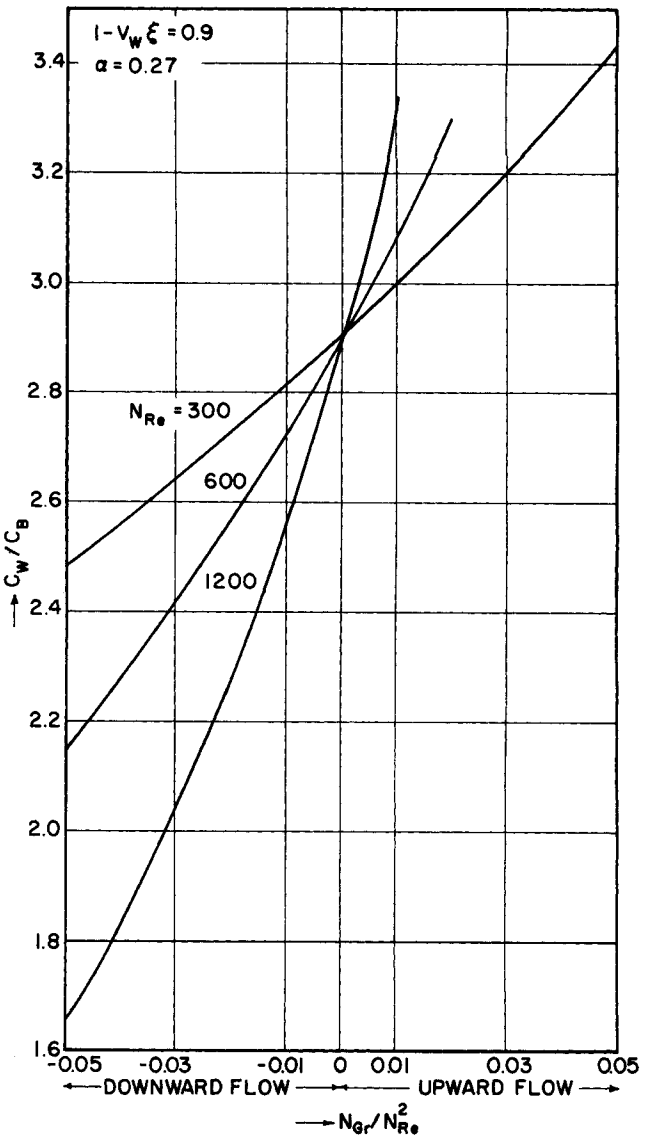

Fig. 14a. Effect of buoyancy on polarization at high values of N_{Re}.

tion from laminar to turbulent flow. Scheele and Hanratty (*17, 18*), on the basis of experimental evidence, indicate that the mechanism of transition occurs through the growth of small disturbances.

The development of the disturbances is implied by the existence of inflexion points in the velocity profile, (Rayleigh's first theorem of instability). Although this criterion strictly holds good only for inviscid flows, some qualitative information, regarding the onset of instability, can be obtained by calculating the inflexion points. Thus by setting $\partial^2 w/\partial\eta^2 = 0$, one obtains from Equations (41) and (58)

$$\frac{\phi_{10}'''(\eta)}{(1-v_w\xi)^2} + \frac{\phi_{20}'''(\eta)}{(1-v_w\xi)^{(2-2/3\,\beta_1)}} = \frac{3}{\dfrac{N_{Gr}}{N_{Re}}} \tag{63}$$

For specified values of $(1 - v_w\xi)$ and N_{Gr}/N_{Re}, the roots of this equation corresponding to η between 0 and 1.0, give the inflexion points. These are plotted in Figures 10 and 11. The existence of inflexion points in viscous flows is a necessary but not a sufficient condition for the onset of instability. The problem of instability in viscous channel flows has been considered very recently by Fu and Joseph (*7*).

The transition to turbulence seems to occur differently in upward and downward flows. For heat transfer, Scheele, et al. (*17, 18*) observed experimentally that in upward flow turbulence occurs when the velocity gradient at the wall becomes zero. The criterion for a zero gradient in the present case is

$$\left(\frac{N_{Gr}}{N_{Re}}\right)_{\text{critical}} = \frac{3}{\left[\dfrac{\phi_{10}''(1)}{(1-v_w\xi)^2} + \dfrac{\phi_{20}''(1)}{(1-v_w\xi)^{(2-2/3\,\beta_1)}}\right]} \tag{64}$$

These values are plotted in Figure 8. On comparing Figures 8 and 10, it is seen that inflexion points exist at much lower N_{Gr}/N_{Re} ratios than those given by Equation (64) at which the transition probably occurs.

For downward flows a similar situation to that in upward flow exists in that two values of N_{Gr}/N_{Re} also exist; these involve first the development of inflexion points and second a flow reversal in the center of the channel. The first of these corresponds to an incipient dimple formation in the center of the flow, and from Equation (58) one obtains

$$\left(\frac{N_{Gr}}{N_{Re}}\right)_{\text{critical}} = \frac{3}{\left[\dfrac{\phi_{10}'''(0)}{(1-v_w\xi)^2} + \dfrac{\phi_{20}'''(0)}{(1-v_w\xi)^{(2-2/3\,\beta_1)}}\right]} \tag{65}$$

by letting $\partial^2 w/\partial\eta^2 = 0$ at the center. These values are plotted in Figure 9. In addition, in downward flow, flow reversal at the center is associated with the condition $w = 0$ at $\eta = 0$ which yields a second criterion

$$\left(\frac{N_{Gr}}{N_{Re}}\right)_{\text{critical}} = \frac{-1.5}{\left[\dfrac{\phi_{10}'(0)}{(1-v_w\xi)^2} + \dfrac{\phi_{20}'(0)}{(1-v_w\xi)^{(2-2/3\,\beta_1)}}\right]} \quad (66)$$

These values are also plotted in Figure 9. A comparison of Figures 9 and 11 indicates that for $\alpha = 0.5$, the inflexion point is first observed close to the dimple formation and with increasing buoyancy it moves towards the wall. This is in qualitative agreement with the observations of Scheele et al. who suggested that disturbances are first observed at the formation of a dimple in the velocity profile. However, for $\alpha = 0.27$, inflection points seem to exist even for values of N_{Gr}/N_{Re} less than the value corresponding to dimple formation. Further there seems to exist a range of the N_{Gr}/N_{Re} ratio, at which two points of inflection occur. On qualitative grounds one might say that disturbances first develop at the formation of a dimple and gradually increase with buoyancy until flow reversal takes place, and this is accompanied by transition to turbulence.

The effect of natural convection on polarization and mass transfer rates is indicated in Figures 12 through 15. Figure 12 shows the variation of polarization with buoyancy in upward and downward flows for different N_{Re} at $\alpha = 0.5$. It can be seen that the effect of buoyancy is to increase polarization in upward flows and decrease it in downward flows. This is what one would expect, since the velocity gradients near the wall (which is proportional to the shear stress) decreases in upward flows and increases in downward flows. Curves are drawn for $N_{Re} = 30$, 60, 120, 300, 600, and 1,200 and care must be exercised when interpreting these plots. For example, at first sight it appears as though polarization increases with increasing N_{Re}. However, it is evident that if we hold the Grashof number constant then $N_{Gr}/N_{Re}^2 = 0.4$ with $N_{Re} = 30$ corresponds to $N_{Gr}/N_{Re}^2 = 0.1$ with $N_{Re} = 60$ and the polarization in the latter case is less than in the former which indicates that polarization decreases with increasing N_{Re} as one would expect.

Figure 13 indicates Sherwood number variation with the buoyancy parameter at different N_{Re} for $\alpha = 0.5$. If one defines a mass transfer coefficient, k_l, by

$$N_s = k_l(c_w - c_B) = D\left.\frac{\partial c}{\partial y}\right|_{y=h} = v_w{}^+ c_w$$

and it follows that

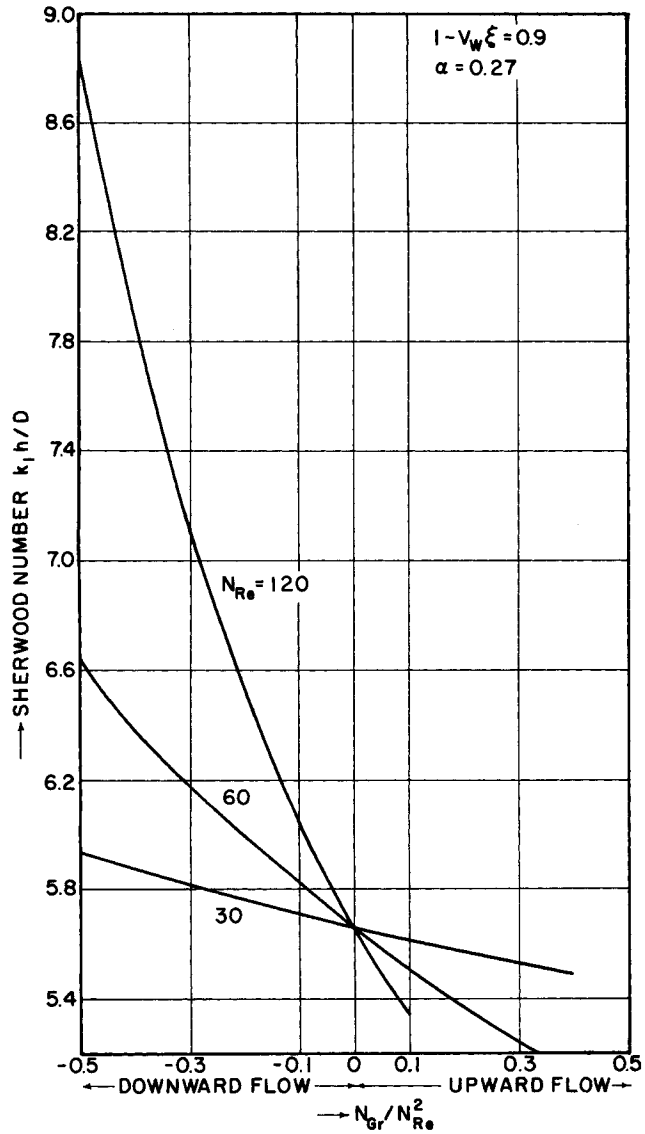

Fig. 15. Effect of buoyancy on Sherwood number for different N_{Re}.

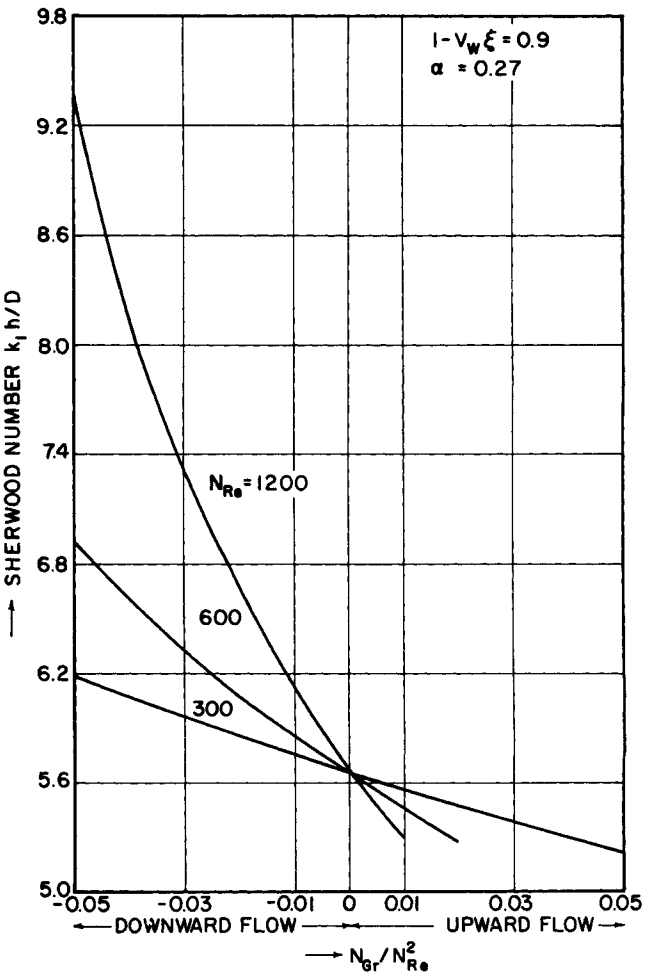

Fig. 15a. Effect of buoyancy on Sherwood number at high N_{Re}.

$$N_{Sh} = \frac{\theta_w}{(\theta_w - \theta_B)\alpha}$$

Sherwood numbers are found to decrease with increasing buoyancy in upward flows and vice versa for downward flows. Figures 14 and 15 illustrate the variation of polarization and mass transfer rates with N_{Gr}/N_{Re}^2 at $\alpha = 0.27$. One can clearly see that the effect of increased flux is to increase buoyancy effects. This occurs because an increase in flux creates greater polarization at the membrane surface and therefore greater density gradients across the flow.

CONCLUSIONS

1. The coupled equations of momentum and diffusion have been solved by using a scheme which employs the buoyancy parameter, N_{Gr}/N_{Re}^2 as the perturbation parameter.
2. Natural convection is found to have a significant influence on the velocity profiles which depends on the direction of flow. In particular, it may be noted that transition to turbulence occurs at much lower values of N_{Gr}/N_{Re} ratio for upward flows than for downward flows. Similar observations have been made by Scheele, et al. (*17*) for heat transfer systems.
3. Mass transfer rates are decreased and therefore polarization increases by buoyancy effects in upward flows providing the flow remains laminar. The opposite is true of downward flows wherein the velocity gradients at the surface are increased by buoyancy and therefore mass transfer rates are increased.
4. Hydrodynamically stable systems would be expected to exist only up to the critical N_{Gr}/N_{Re} ratios. It is also worth noting that in downward flows the system tends to remain stable over a wider range of the N_{Gr}/N_{Re} ratio when compared to upward flows.
5. The principal difference between the analysis of the buoyancy effects created by mass rather than heat transfer, is that the boundary conditions in mass transfer are such that simple similarity transformations of the kind encountered elsewhere (*6, 21*) do not exist.

Also, mass transfer systems of the reverse osmosis type involve the additional parameter α. The role of this parameter is to increase buoyancy effects with decreasing values of α, due to the higher polarization involved.

ACKNOWLEDGMENT

This work was supported by the Office of Saline Water, United States Department of Interior.

NOTATION

A = membrane consant defined by Equation (6)
B = defined by Equation (16)
C_B = bulk concentration of salt
c_s = salt concentration
c_{s0} = salt concentration at the inlet of channel
c_w = salt concentration at brine membrane interface
D = molecular diffusion coefficient
E = defined by Equation (49)
F = defined by Equation (17)
h = channel half width
k_l = mass transfer coefficient
N_{Re} = inlet Reynolds number hU_{b0}/ν
N_{Gr} = Grashof number $h^3g\beta c_{s0}/\nu^2$
N_{Fr} = Froude number U_{b0}^2/hg
N_{Pe} = inlet Peclet number hU_{b0}/D
N_{Sh} = Sherwood number k_lh/D
N_s = salt flux through the wall
p^+ = dimensional pressure
p_0^+ = pressure at the standard state
p = dimensionless pressure $p^+ - p_0^+/\rho_0 U_{b0}^2$
N_{Rew} = wall Reynolds number defined by Equation (27*a*)
U = axial velocity
U_m = mean velocity of flow
U_{b0} = inlet bulk velocity
v^+ = transverse velocity
v = dimensionless transverse velocity v^+/U_{b0}
v_w = dimensionless transverse velocity at the membrane surface
v_w^+ = wall velocity
w = dimensionless axial velocity, U/U_{b0}
x = axial coordinate
y = transverse coordinate

Greek Letters

α = reciprocal of the wall Peclet number
β = coefficient of expansion defined by Equation (2*a*)
β_n = eigenvalues of Equation (29)
ΔP = applied pressure drop across the membrane interface
ϵ = perturbation parameter N_{Gr}/N_{Re}^2
η = dimensionless transverse coordinate y/h
θ = dimensionless concentration c_s/c_{s0}
ξ = dimensionless axial coordinate x/h
π_p = osmotic pressure corresponding to product solution
π_w = osmotic pressure at brine membrane interface
ρ = density
$\rho(\eta)$ = weighting function; Equation (55*b*)
σ = variable defined by Equation (47)
ϕ = defined by Equation (35)
ψ = dimensionless stream function defined by Equation (13)
$\chi_\eta(\xi)$ = axial eigenfunction defined by Equation (55)

LITERATURE CITED

1. Bartels, C. F., and R. V. Churchill, *Bull. Am. Math. Soc.* **48**, 276 (1942).
2. Berman, A. S., *J. Appl. Phys.*, **24**, 1232 (1953).
3. Brian, P. L. T., *Ind. Eng. Chem. Fundamentals*, **4**, 439 (1965).
4. Brown, C. K., W. H. Gauvin, *Can. J. Chem. Eng.*, **43**, 306 (1965).
5. Ibid., 313 (1965).
6. Carter, L. F., and W. N. Gill, *AIChE J.*, **10**, 330 (1964).
7. Fu, T. S., and D. D. Joseph, *Phys. Fluids*, to be published.
8. Gill, W. N., and E. Del Casal, *AIChE J.*, **8**, 513 (1962).
9. ———, Chi Tien, and D. W. Zeh, *Ind. Eng. Chem. Fundamentals*, **4**, 433 (1965).
10. ————, *Int. J. Heat Mass Transfer*, **9**, 907 (1966).
11. Gill, W. N., D. W. Zeh, and Chi Tien, *AIChE J.*, **12**, 1141 (1966).
12. Hanratty, T. J., E. M. Rosen, and R. L. Kabel, *Ind. Eng. Chem.*, **50**, 815 (1958).
13. Merten, U., H. K. Lonsdale, R. L. Riley, *Ind. Eng. Chem. Fundamentals*, **3**, 210 (1964).
14. Ramanadhan, K., MS thesis, Clarkson College Tech., Potsdam, New York (1968).
15. Reejsinghani, N. S., W. N. Gill, and A. J. Barduhn, *AIChE J.*, **12**, 916 (1966).
16. Ibid., **14**, 100 (1968).
17. Scheele, G. F., E. M. Rosen, and T. J. Hanratty, *Can. J. Chem. Eng.*, **38**, 67 (1960).
18. ———, and T. J. Hanratty, *AIChE J.*, **9**, 183 (1963).
19. ————, *J. Fluid Mech*, **14**, 244 (1962).
20. Sherwood, T. K., P. L. T. Brian, R. E. Fisher, L. Dresner, *Ind. Eng. Chem. Fundamentals*, **4**, 113 (1965).
21. Sparrow, E. M., and J. L. Gregg, *J. Appl. Mech.*, **26**, 133 (1959).
22. Srinivasan, S., Chi Tien, and W. N. Gill, *Chem. Eng. Sci.*, **22**, 417 (1967).

Manuscript received April 10, 1968; revision received June 17, 1968; paper accepted June 26, 1968.